

## Dissolved oxygen as a tracer for intermediate water mixing characteristics in the Indian Ocean

S. Ramesh<sup>1,\*</sup>, G. A. Ramadass<sup>1</sup>,  
M. Ravichandran<sup>2</sup> and M. A. Atmanand<sup>1</sup>

<sup>1</sup>National Institute of Ocean Technology (MoES),  
Chennai 600 100, India

<sup>2</sup>Indian National Centre for Ocean Information Services (MoES),  
Hyderabad 500 055, India

**The mixing characteristics of intermediate water at the Central Indian Ocean Basin (CIOB) and the Arabian Sea using dissolved oxygen (DO) as a tracer were studied. Only a few datasets are available in the literature for north–south mixing in this region. Our studies using DO sensor mounted on a remotely operated vehicle in comparison with array for real-time geostrophic oceanography (ARGO) reveal the influence of sub-Antarctic mode water (SAMW) in the study region. Reduction in second oxygen maximum concentration anomaly from south to north may be due to very low concentrated oxygen minimum zone in the Arabian Sea and influence of Red Sea water and the Persian Gulf water. We observed second oxygen maximum concentration at a depth of 300–700 m at CIOB from 150 to 220  $\mu\text{M}$ , compared to the Arabian Sea profiles in the 25–40  $\mu\text{M}$  range with peak value at a depth at 450 m. The present study highlights the usage of high-resolution DO data as tracer for intermediate water circulation in the Indian Ocean and also shows the influence of SAMW up to 8°N along 75°E.**

**Keywords:** Dissolved oxygen, intermediate water, mixing characteristics, tracer.

CIRCULATION and mixing of intermediate water in deep ocean basins at the depth range 150–200 to 1000 m play a vital role in controlling nutrient availability, thermocline, freshwater input mixing, salinity distribution, dissolved oxygen (DO) concentration, carbon budgets and global circulation<sup>1,2</sup>. This zone plays a significant role in the upward vertical migration of numerous species to the highly productive photic zone and also in the downward migration of carbonates to bathypelagic zone. Occurrence of steep physico-chemical gradient at mesopelagic zone by following the pattern of thermocline, pycnocline and halocline creates turbulence in circulation pattern and also causes overturning phenomenon. Existence of zonal asymmetry in the intensity of diapycnal mixing and upwelling in the Indian Ocean had been discussed extensively<sup>3–5</sup>. Studies on circulation in the Central Indian Ocean Basin (CIOB) highlight the westward-flowing south equatorial current (SEC) as the permanent circulation

feature<sup>6–9</sup> apart from intermediate water mixing by sub-Antarctic mode water (SAMW)<sup>10,11</sup>.

Variation in vertical profile of DO in ocean basins is classically explained by an advection–diffusion model considering two sources, one, from the deep layers by freshwater mixing and the other from the surface layers by air–sea interaction<sup>12</sup>. When we consider circulation mechanism for oxygen availability, abyssal circulation transports oxygen from the North Atlantic and the Antarctic Sea to deep layers of the Indian and Pacific Oceans via the Antarctic circumpolar current (ACC). Very low O<sub>2</sub> concentration in the northern portion of the deep basin when compared to CIOB may be due to mixing with very low O<sub>2</sub> concentration water in the region, a result of high respiration rates caused by high rates of sinking organic matter formed in productive Arabian Sea surface waters.

Antarctic bottom water (AABW) occupies the deepest parts of the ocean<sup>13</sup> and it is observed to penetrate northward into the Atlantic, Indian and Pacific Oceans through deep passages in the mid-ocean ridge system. The SEC, in general, extends between 10°S and 16°S and exhibits seasonal (north–south) shifts with its northern boundary moving up to 4°S during southern winter<sup>6,14</sup>.

Vertical flow of water through conveyor belt circulation mechanism takes high concentration of oxygen to deeper waters. It is reported that oxygen might be consumed within the ocean by heterotrophic processes and the ocean has no internal oxygen sources<sup>15</sup>. Therefore, DO concentration in the interior of an ocean reflects a balance between supply through circulation and loss through respiration. DO has been effectively used as tracer to track water types, movement of water masses and to monitor global carbon cycle<sup>15–17</sup>. Most of the studies on circulation phenomenon in the Indian Ocean deal with mixing characteristics in segregated zonal patches such as Indonesian through-flow<sup>9</sup>, Agulhas current<sup>18,19</sup>, Somali current<sup>20,21</sup>, SAMW<sup>10</sup> and Red Sea water<sup>22</sup>. The present study brings out the mixing phenomenon of DO by SAMW in the south to north direction from CIOB to the Arabian Sea.

To understand variability and mixing of DO in the north–south direction, observations were made in vertical cross-section across equatorial region in Indian Ocean from 13°S to 8°N lat. along 75°E long. The study deals with the observed DO concentration, water temperature and salinity profiles collected from the Indian Ocean regions up to 5289 m water depth. The datasets were made from surface water mass to 2000 m depth. Data were collected in real time from scientific payload attached to a remotely operated vehicle (ROV), ROSUB 6000, developed by the National Institute of Ocean Technology (NIOT), Chennai, and were compared with profiles from ARGO floats in the nearby region. ROSUB 6000 is a deep-water work-class ROV connected with scientific payloads such as DO sensor (Aanderaa 3830), sound velocity profiler (Mini SVP) and conductivity sensor

\*For correspondence. (e-mail: sramesh@niot.res.in)

(Aanderaa 3919) for real-time high-resolution data collection<sup>23,24</sup>. Most of the earlier similar observations were based on CTD casting with self-recording pre-programmed depth-controlled data acquisition and the observations were viewed using deck unit. The present study is based on the high-resolution information from a sensor with <25 sec settling time without restriction on memory devices and continuous power availability from ROV. During each deployment, scientific sensors were calibrated according to set procedures and data were compared during down-cast and up-cast time for repeatability. Data collected from the sensors were in text format with tag details of position, time, depth, DO, conductivity, water temperature, salinity, sound velocity, etc. For the present study the data collected from the Arabian Sea, equatorial regions and CIOB are compared and representative graphs are presented. Data collected from ARGO floats deployed in the Arabian Sea and equatorial waters of the Indian Ocean, as a part of the ARGO programme were also used for comparison and to corroborate the results obtained using ROSUB 6000. Even though profiles of ROSUB-ROV are available up to a maximum depth of 5289 m from CIOB, for comparison and interpretation of mesopelagic water and also owing to ARGO data limitations (<2000 m), all the profiles were made for depths up to 1600 m. Location details and the study region of ROSUB 6000 and ARGO profiles are shown in Figure 1. Data collected from the study region using ROSUB 6000 for the interpretation of SAMW are given in Table 1 for the depth range up to 1000 m.

Variation in concentration of DO indicates dilution effect due to mesopelagic water circulation in mid-depth water masses in the southern hemisphere ocean under the influence of SAMW and Antarctic intermediate water (AAIW)<sup>1</sup>. Apart from prevailing circulation currents in the study regions, intermediate water movement is controlled by the deep-sea geomorphologic features such as N-S trending Laccadive-Maldives ridge, Carlsberg ridge

in the Arabian Sea and Coriolis force effect between the southern and northern hemispheres. On the basis of geographical locations of the data collection site, the sites can be classified as Arabian Sea zone, equatorial waters and CIOB regions. Even though profiles collected are sporadic when compared to spatial extent of the study region, data clearly reflect the characteristic trend to understand the mixing phenomenon, especially in the south to north direction.

DO profiles from the study region (Figure 2) show high concentration up to 60 m water depth, indicating surface water mixing zone similar to the observation of shallow mixed layer (MLD  $\leq$  60 m)<sup>1</sup>. Underneath the

**Table 1.** Dissolved oxygen data collected using ROSUB 60000 from the Indian Ocean

Depth (m)	Dissolved oxygen concentration ( $\mu\text{mol}$ )				
	ROSUB 0110	ROSUB 0210	ROSUB 0310	ROSUB 0410	ROSUB average
-0.2	284.2	305.3	312.8	314.4	304.2
-10.2	299.3	307.2	309.2	312.6	307.1
-25.4	311.4	308.5	309.3	312.4	310.4
-50.4	313.0	303.5	312.0	313.1	310.4
-75.3	303.0	242.8	303.0	303.3	288.0
-100.6	194.3	166.2	213.9	221.2	198.9
-125.4	68.9	121.7	131.9	199.9	130.6
-150.3	23.7	119.9	138.1	192.4	118.5
-175.3	13.8	113.3	134.1	183.5	111.2
-200.2	12.0	124.8	129.6	160.9	106.8
-225.7	10.4	138.0	124.7	135.8	102.2
-250.5	8.4	148.7	115.9	135.2	102.1
-275.5	8.4	137.2	111.2	136.1	98.2
-300.4	8.6	119.8	111.6	139.3	94.8
-325.4	11.4	114.0	116.9	133.8	94.0
-350.2	14.5	116.3	131.1	136.5	99.6
-375.4	21.8	134.6	135.8	152.3	111.1
-400.7	24.8	146.9	173.6	185.1	132.6
-425.4	22.8	139.9	188.4	203.0	138.5
-450.3	24.5	139.1	166.8	211.2	135.4
-475.3	26.6	148.5	146.1	202.6	131.0
-500.6	26.2	134.1	128.6	180.9	117.5
-550.5	24.8	123.6	113.6	160.6	105.6
-575.2	24.3	117.4	108.6	169.1	104.8
-600.3	23.2	102.5	109.1	161.6	99.1
-625.4	20.7	91.2	109.4	147.4	92.1
-650.3	21.3	84.5	108.1	140.1	88.5
-675.3	22.5	75.5	107.7	133.2	84.8
-700.1	23.0	77.9	106.8	126.1	83.5
-725.3	24.3	79.9	106.4	124.4	83.7
-750.6	26.0	82.2	107.8	122.5	84.6
-775.5	27.3	83.0	110.0	121.6	85.4
-800.7	28.5	82.1	111.2	123.3	86.3
-825.8	28.6	77.8	112.4	123.6	85.6
-850.6	29.9	76.4	113.8	122.3	85.6
-875.3	32.7	77.6	114.9	120.3	86.4
-900.6	34.4	79.2	116.0	119.1	87.2
-925.9	36.7	80.3	116.8	118.9	88.2
-951.0	38.5	80.5	117.5	119.9	89.1
-975.7	41.8	80.5	118.6	119.9	90.2
-1000.7	45.0	78.0	119.2	120.4	90.7

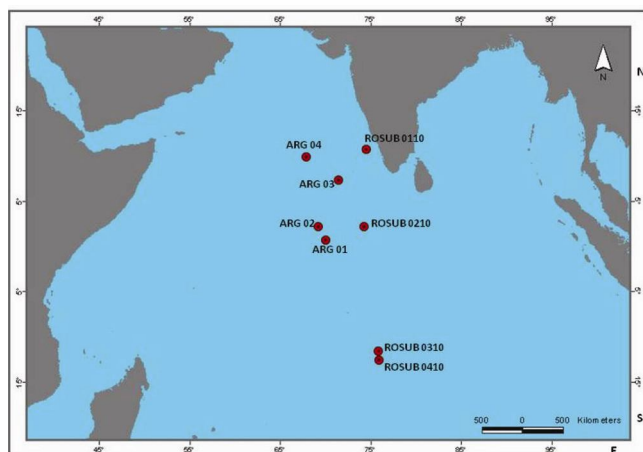


**Figure 1.** Locations of the profiles in the Indian Ocean.

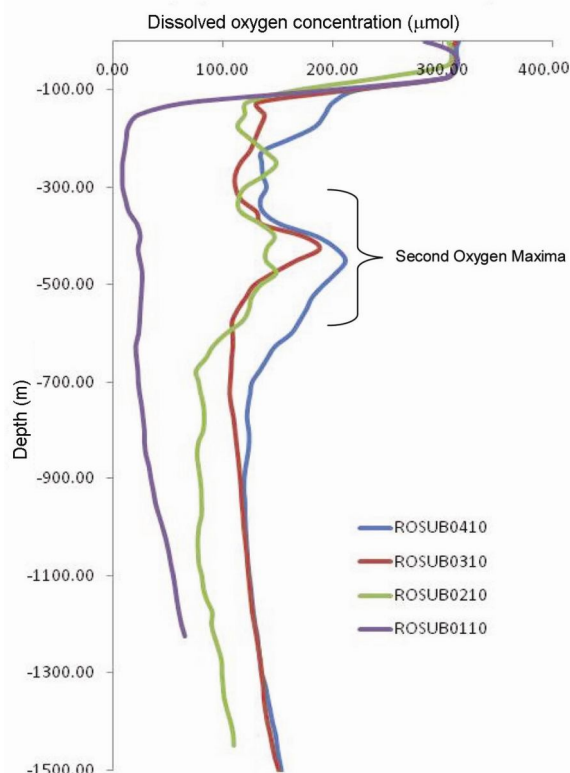


**Figure 2.** Dissolved oxygen concentration profile from the Indian Ocean.

mixing zone, oxygen minimum zone (OMZ) is recorded in the profiles, wherein DO concentration is reduced from 290 to 150  $\mu\text{M}$  in CIOB and in the equatorial regions. In the Arabian Sea region, OMZ is recorded with DO value of 275–25  $\mu\text{M}$ . Recorded OMZ zone in the Arabian Sea profile is almost similar to the earlier observations<sup>25,26</sup>. Very low oxygen content in OMZ in the Arabian Sea profiles in comparison to CIOB and equatorial region might be due to the long residence time of upwelled water and the existence of warm, low-salinity waters<sup>25</sup>. Meridional overturning circulation (MOC) studies show that long residence time (90 years) of water plays a key role in explaining the oxygen depletion in the Indian Ocean<sup>27</sup>.

Arabian Sea intermediate waters DO profile shows distinctive anomaly from 25 to 40  $\mu\text{M}$  with peak value at a depth of 450 m (Figure 2). Physico-chemical factors which influence the concentration of DO in ocean basins are temperature due to cold freshwater inputs due to melting of polar ice and mixing by SAMW, cold freshwater input, increase of pressure by depth, partial pressure and density variation due to dissolved solid loading. To find out the variation in the physico-chemical factors, water temperature, conductivity, salinity and density were measured with *in situ* probes to identify influencing parameter. Results indicate that the contribution of the observed anomaly in DO is not site-specific and it is the net product of global intermediate water circulation phe-

nomena like SAMW. Since the profiles are taken in the north–south transect along 75°E, the results clearly brings out mixing characteristics of DO from CIOB to the equator and further north towards the Arabian Sea, i.e. very low oxygenated water in the Arabian Sea is mixing with higher concentration of oxygen from CIOB at the mesopelagic zone. The resultant profile of up to 5289 m for DO from CIOB clearly shows the second oxygen maximum and general increasing trend of DO observed up to 2000 m water depth, which stabilizes to 200  $\mu\text{M}$  with water temperature reaching 1.6°C at 5289 m water depth (Figure 3).

The anomaly observed as second oxygen maximum from 13°S to 8°N along 75°E in intermediate waters (450 m) might be due to Sverdrup's Indian Ocean central water<sup>28</sup>, i.e. SAMW. Intermediate water in the Indian Ocean at 400–600 m depths at 32°S had recorded high oxygen concentration of 234–245  $\mu\text{M}$  (ref. 29) and also in the Atlantis II section at 18°S in the depth range 400–500 m (ref. 2). Studies at 15–30°S in north–south direction had reported coldest and densest bottom water with higher oxygen content at a depth of 500–1500 m (ref. 16). The present observation of second oxygen maximum can be traced from CIOB up to the Arabian Sea profiles at a depth range of 450 m.

Studies on meridional overturning cell (MOC) in the Pacific and Indian Oceans are well-established in the literature<sup>30</sup>. This cell is primarily controlled by the wind, but thermohaline processes determine its detailed structure. The present observation of second DO maximum from CIOB to Arabian Sea at a depth range 275–750 m might also be a resultant of MOC. Results show that SAMW does not stop at the equatorial region, it further carries the high-oxygenated water towards the Arabian Sea up to the observed location of 8°N, and needs to be studied further with close grid connecting profiles. Anomalies observed as second oxygen maximum at the intermediate depth (275–750 m) in the Arabian Sea and CIOB are comparable, but the concentration levels are different: 125–150  $\mu\text{M}$  and 25–40  $\mu\text{M}$  respectively.

Comparison study highlights that the profiles from ROSUB and ARGO datasets demonstrate the influence of Carlsberg ridge for the intermediate water mixing. It shows that concentration of DO is less on the western side of Carlsberg ridge region when compared to the eastern side of the study region. It might be due to the effect of Somali current in the west and Red Sea current in the east from the northern region. Comparison of DO profiles collected at 2°S from ROSUB and ARGO along with salinity clearly shows freshwater input indicated by salinity reduction in mid-depth layer (Figure 4). Earlier studies recorded<sup>31</sup> that Red Sea and Northern Arabian Sea intermediate waters do not penetrate below 1000 m, and also lose their identity as they cross the equator by mixing with low-salinity Indonesian through-flow waters or by intermediate SAMW. Further detailed studies in

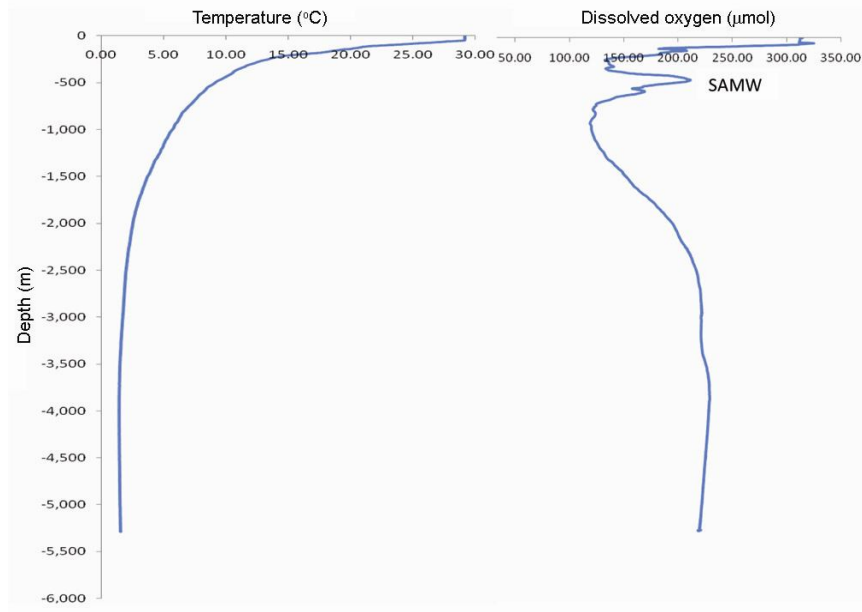


**Figure 3.** Deep water profile of temperature and dissolved oxygen data collected up to 5289 m water depth at CIOB (ROSUB 0410).

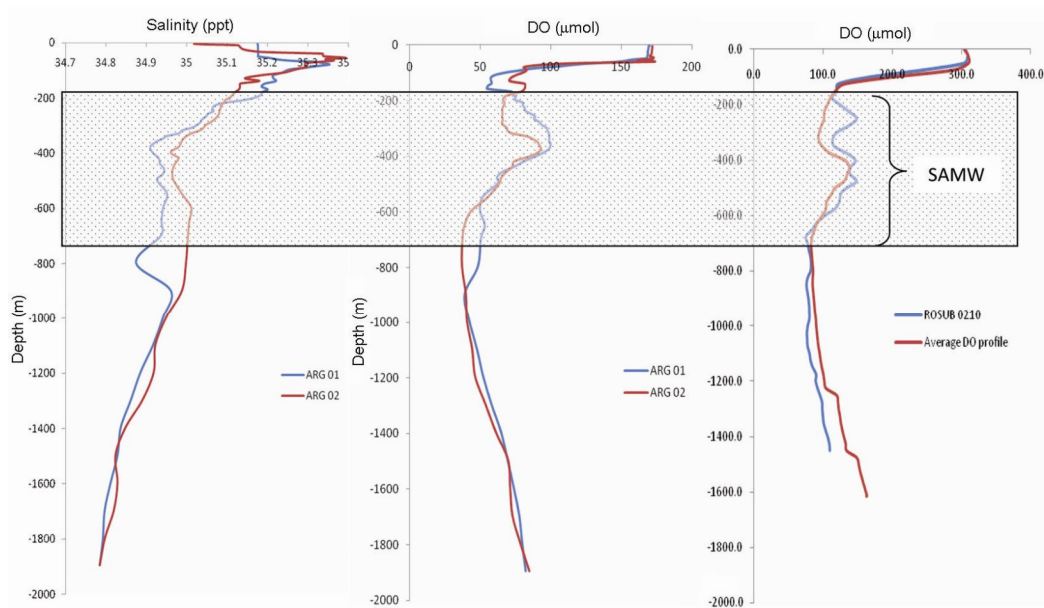


**Figure 4.** High oxygen correlation with low salinity water (ARG, ARGO floats data; ROSUB, Data collected from ROV; SAMW, Sub-Antarctic mode water mixing area).

these regions in longitudinal way will resolve the mixing zonation in continental regions due to the influence of deep water circulation.

DO, salinity and temperature datasets collected from ROSUB 6000-based ROV are analysed and compared with ARGO floats data. Results from the data show clear demarcation of second oxygen maximum and its dilution towards north from CIOB to the Arabian Sea. There are regions of mixing and dilution at the equatorial Indian Ocean which control the distribution of DO content in

these waters. Based on the  $T-S$  and  $T-DO$  plot (Figures 5 and 6), the influence of SAMW is clearly reflected in the collected profiles similar to the earlier observations<sup>32,33</sup>.  $T-S$  plots were drawn based on the nearby ARGO profiles data and they show influence of the Arabian Sea water pattern in ARG 04 profile; equatorial Indian Ocean water trend is observed in ARG 01 and 02. ARG Near ROSUB 0310 shows low salinity trend of freshwater mixing when compared to northern basin data. Plots were compared with the ocean water mixing curve established

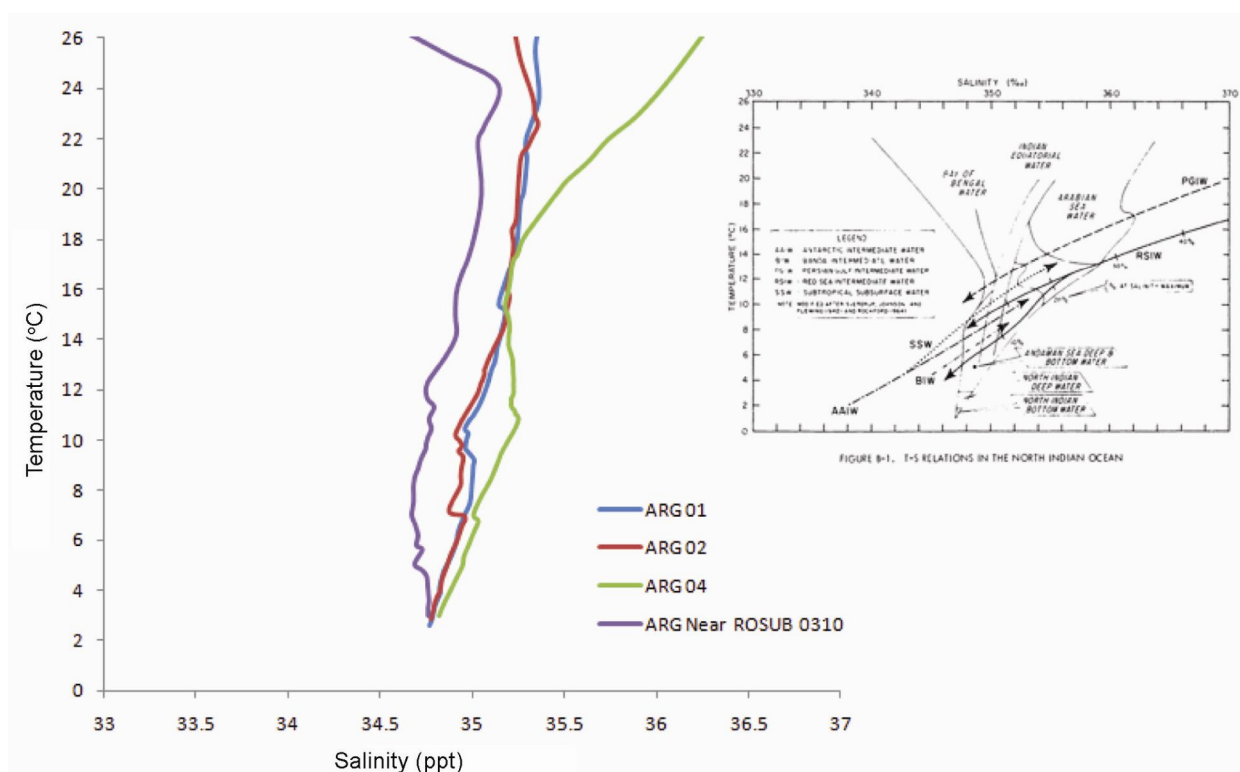


Figure 5. Temperature–salinity plot of study region in comparison with International Ocean Expedition water mixing curve<sup>32</sup>.

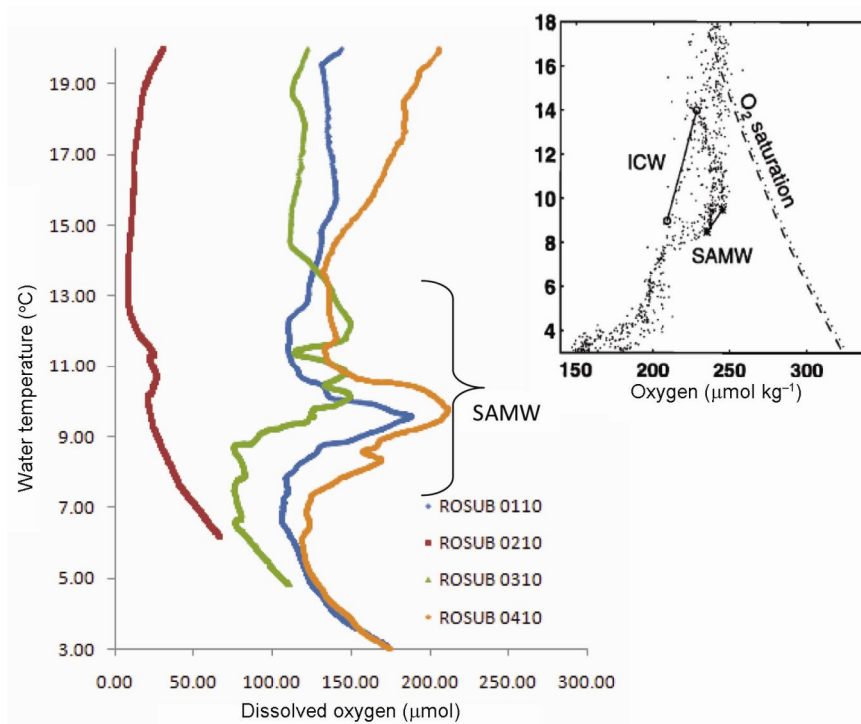


Figure 6. Temperature–DO plot showing the influence of SAMW. (Inset) For comparison<sup>33</sup>.

by earlier researchers<sup>32</sup> (Figure 5). As envisaged by earlier studies<sup>10,34</sup>, results from the present observations also indicate that the combination of fresher, colder and

denser SAMW across southern Indian Ocean basin results in subtropical distribution of SAMW up to the Arabian Sea. The present study on mesopelagic zone variation of

DO from high-resolution datasets and observed second oxygen maximum characteristics in longitudinal profile in the Indian Ocean, tracks the influence of SAMW up to 8°N in the study region which had been indicated earlier up to 15°S (ref. 16). Temperature versus DO plot (Figure 6) from ROSUB datasets shows clear anomaly due to influence of SAMW reported earlier<sup>33</sup>. To further improve our understanding, with technological advancement in terms of floating probes and deep-water data collection capability, it is possible to track in closed grid interval the water movement using DO as a tracer. Further detailed studies in these regions in longitudinal way are needed to resolve the mixing zonation in continental regions due to the influence of deep water circulation.

1. Sloyan Bernadette, M., Lynne, M., Talleu, D., Teresa, K., Chereskin, F. R. and James, H., Antarctic intermediate water and subantarctic mode water formation in the Southeast Pacific: the role of turbulent mixing. *J. Phys. Oceanogr.*, 2010, **40**, 1558–1574.
2. Warren, B. A., The deep water of the Central Indian Basin. *J. Mar. Res. (Suppl.)*, 1982, **40**, 823–860.
3. de Sousa, S. N., Sardessai, S. D., Ramesh Babu, V., Murty, V. S. N. and Gupta, G. V. M., Chemical characteristics of Central Indian Basin waters during the southern summer. *Deep Sea Res. II*, 2001, **48**, 3343–3352.
4. McCarthy, M. C. and Talley, L. D., Three-dimensional potential vorticity structure in the Indian Ocean. *J. Geophys. Res.*, 1999, **104**, 13251–13267.
5. Srinivasan, A., Rooth, C. G. H., Top, Z. and Olson, D. B., Abyssal upwelling in the Indian Ocean: radiocarbon diagnostics. *J. Mar. Res.*, 2000, **58**, 755–778.
6. Murty, V. S. N. *et al.*, Seasonal variability of upper-layer geotropic transport in the tropical Indian Ocean during 1992–1996 along TOGA-I XBT track lines. *Deep Sea Res. I*, 2000, **47**, 1569–1582.
7. Peter, B. N. and Mizuno, K., Annual cycle of steric height in the Indian Ocean estimated from thermal field. *Deep-Sea Res. I*, 2000, **47**, 1351–1368.
8. Bahulayan, N. and Shaji, C., Diagnostic 3-D circulation in the Arabian Sea and western equatorial Indian Ocean: result of monthly sea surface topography. *Proc. Indian Natl. Sci. Acad., Part A*, 1996, **62**, 325–347.
9. Wyrtki, K., *Oceanographic Atlas of the International Indian Ocean Expedition*, Nat. Sci. Found., Washington, DC, 1971, p. 531.
10. McCartney, M. S., Subantarctic mode water. *Deep Sea Res. (Suppl.)*, 1977, **24**, 103–119.
11. Warren, B. A., TransIndian hydrographic section at latitude 181°S: property distributions and circulations in the South Indian Ocean. *Deep-Sea Res. I*, 1981, **28**(A8), 759–788.
12. van Geen, A., Smethie Jr, W. M., Horneman, A. and Lee, H., Sensitivity of the North Pacific oxygen minimum zone to changes in ocean circulation: a simple model calibrated by chlorofluorocarbons. *J. Geophys. Res.*, 2006, **111**(C10004), 1–11.
13. Kerr, A., Mata, M. M. and Garcia, C. A. E., On the temporal variability of the Weddell sea deep water masses. *Antarct. Sci.*, 2009, **21**, 383–400.
14. Murty, V. S. N., Savin, M., Ramesh Babu, V. and Suryanarayana, A., Seasonal variability in the vertical current structure and kinetic energy in the Central Indian Ocean Basin. *Deep-Sea Res. II*, 2001, **48**, 3309–3326.
15. Kortzinger, A., Schimanski, J., Send, U. and Wallace, D., The ocean takes a deep breath. *Science*, 2004, **306**, 1337.
16. Reid, J. L., On the total geostrophic circulation of the Indian Ocean: flow patterns, tracers, and transports. *Prog. Oceanogr.*, 2003, **56**, 137–186.
17. Toggweiler, J. R. and Key, R. K., Thermohaline circulation. In *Encyclopedia of Ocean Sciences*, 2001, pp. 2941–2947.
18. Jacobs, S. S. and Georgi, D. T., Observations on the southwest Indian/Antarctic Ocean. *Deep-Sea Res. (Suppl.)*, 1977, **24**, 43–84.
19. Beal Lisa, M., Wilhelmus, P. M., De Ruijter, Biastoch, A. and Zahn, R., On the role of the Agulhas system in ocean circulation and climate – SCOR/WCRP/IAPSO Working Group 136. *Nature*, 2011, **472**, 429–436.
20. Düing, W. and Schott, F., Measurements in the source region of the Somali current during the monsoon reversal. *J. Phys. Oceanogr.*, 1978, **8**, 278–289.
21. Schott, F. A. and McCreary, J. P., The monsoon circulation of the Indian Ocean. *Prog. Oceanogr.*, 2001, **51**, 1–123.
22. Grundlingh, M. L., Occurrence of Red Sea water in the southwestern Indian Ocean. *J. Phys. Oceanogr.*, 1985, **15**, 207–212.
23. Ramadass, G. A. *et al.*, Deep-ocean exploration using remotely operated vehicle at gas hydrate site in Krishna–Godavari basin, Bay of Bengal. *Curr. Sci.*, 2010, **99**, 809–815.
24. Manecius Selvakumar, J. *et al.*, Technology tool for deep ocean exploration – remotely operated vehicle. In Proceedings of the 20th International Offshore and Polar Engineering Conference, Beijing, China, 2010, pp. 206–212.
25. Naqvi, S. W. A., Oxygen deficiency in the Northern Indian Ocean, *Suplemento Gayana*, 2006, **70**, 53–58.
26. Helly, J. J. and Levin, L. A., Global distribution of naturally occurring marine hypoxia on continental margins. *Deep-Sea Res. I*, 2004, **51**, 1159–1168.
27. Drijfhout, S. S. and Naveira, G. A. C., The zonal dimension of the Indian Ocean meridional overturning circulation. *J. Phys. Oceanogr.*, 2008, **38**, 359–379.
28. Sverdrup, H. U., Johnson, M. W. and Fleming, R. H., *The Oceans: Their Physics, Chemistry and General Biology*, Prentice-Hall, NJ, 1942, p. 1087.
29. Toole, J. M. and Warren, B. A., A hydrographic section across the subtropical South Indian Ocean. *Deep-Sea Res. I*, 1993, **40**(10), 1973–2019.
30. Nof, D., Is there a meridional overturning cell in the Pacific and Indian Oceans? *J. Phys. Oceanogr.*, 2002, **32**, 1947–1959.
31. Piotrowski, A. M., Banakar, V. K., Scrivner, A. E., Elderfield, H., Galy, A. and Dennis A., Indian Ocean circulation and productivity during the last glacial cycle. *Earth Planet. Sci. Lett.*, 2009, **285**, 179–189.
32. Karstensen, J. and Tomczek, M., Age determination of mixed water masses using CFC and oxygen data. *J. Geophys. Res.*, 1998, **103**, 18599–18609.
33. Don, F. F. and Paul, B. J., The sound velocity structure of the North Indian Ocean. Technical Report, US Naval Oceanographic Office, 1972, TR-231, p. 98.
34. McCartney, M. S., The subtropical recirculation of mode waters. *J. Mar. Res.*, 1982, **40**, 427–464.

ACKNOWLEDGEMENTS. We thank the Ministry of Earth Sciences, New Delhi for providing financial support to develop ROSUB 6000 under the Poly Metallic Nodule and Gas Hydrate programme. We also thank the ROSUB team and Manager, Vessel Management Cell, NIOT, Chennai for their support during ROSUB 6000 sea trials.

Received 12 April 2013; revised accepted 23 October 2013